Langmuir

Article

pubs.acs.org/Langmuir

# Hybrid Polyethylenimine and Polyacrylic Acid-Bound Iron Oxide as a Magnetoplex for Gene Delivery

Shuo-Li Sun, Yu-Lun Lo, Hsing-Yin Chen, and Li-Fang Wang*

Department of Medicinal & Applied Chemistry, Kaohsiung Medical University, Kaohsiung 80708, Taiwan

Supporting Information

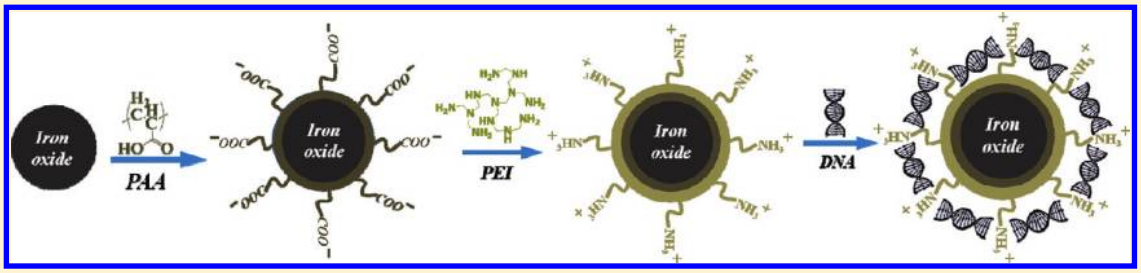


**ABSTRACT:** Low transfection efficiency is always an issue when cationic polymers are used as a nonviral gene vector in the physiological condition, especially in the presence of proteins. A cationic magnetic nanoparticle (MNP) may be an alternative to solve this problem because a magnetic field can help to attract the MNP and internalize it into cells. The aim of this study was to determine the potency of polyethylenimine (PEI)-decorated MNPs for efficiently complexing and delivering plasmid DNA *in vitro* with the help of a magnetic field. PEI is associated with poly(acrylic acid)-bound superparamagnetic iron oxide (PAAIO) through electrostatic interactions (PEI-PAAIO). PEI-PAAIO formed stable polyplexes with pDNA in the presence and absence of 10% fetal bovine serum (FBS) and could be used for magnetofection. The effect of a static magnetic field on the cytotoxicity, cellular uptake, and transfection efficiency of PEI-PAAIO/pDNA was evaluated with and without 10% FBS. Magnetofection efficacy in HEK 293T cells and U87 cells containing 10% FBS was significantly improved in the presence of an external magnetic field. The amount of internalized iron was quantitatively measured using an inductively coupled plasma-optical emission spectrometer and directly visualized using Prussian blue staining. The internalized pDNA was visualized using a confocal laser scanning microscope.

## 1. INTRODUCTION

Magnetofection is a method of transfecting cells in culture; it is defined as magnetically enhanced delivery to cultured cells of DNA, siRNA, or nucleic acids associated with magnetic nanoparticles (MNPs). Since the first presentation in 2000[1] on using magnetofection for gene delivery, the potential of this method to improve the delivery of pDNA[2,3] and siRNA[4−6] in transgene expression has been extensively discussed in the literature. We previously[7,8] synthesized a highly water-soluble, stable, and nontoxic poly(acrylic acid)-decorated iron oxide (PAAIO) for multifaceted biomedical applications. Here, we explored the potential of PAAIO as an MNP core for gene delivery. PAAIO coated with polyethylenimine (PEI-PAAIO) can be used for magnetofection. The improved gene transfection efficiency is expected upon imposed magnetic fields because of the superparamagnetism of PAAIO. The merits of using PAAIO as a magnetic core can be summarized thus: (a) PAAIO is synthesized through a simple one-pot reaction and a highly water-soluble MNP is obtained. Most of the MNPs are synthesized in organic media and transferred to the water phase using either a ligand exchange[9] or a coating material.[10] This may cause some toxicity because organic solvents and surfactants are used. (b) The cytotoxicity is lower than that caused when $Fe_3O_4$ is used.[7] (c) The MNPs are stable in aqueous solution for longer than 9 months.[8] (d) The negatively charged surface of the PAAIO readily forms a stable complex with the positively charged PEI.

PEI, one of the most efficient polymeric nonviral gene delivery vectors, has been extensively studied,[11−13] especially with MNPs for siRNA delivery.[14−19] Transfection efficiency using a precipitated iron oxide surface coated with PEI (PEI-Mag2) was improved up to several 1000-fold compared with using nonmagnetic gene vectors.[20]

Recently, MNPs have been prepared *in situ* in the presence of ferrous salts and hyperbranched PEI (HPEI) with different molecular weights.[4] The combined use of HPEI-decorated MNPs (HPEI-Mag) and pure HPEI dramatically improved gene transfection compared with using HPEI-Mag or HPEI as a gene vector alone. Branched PEI has also been chemically conjugated on thermally cross-linked superparamagnetic iron oxide nanoparticles (TCL-SPION) to transfect a therapeutic gene in primary vascular endothelial cells.[21] PEI-decorated TCL-SPION via a chemical conjugation showed better serum stability than that prepared using physical electrostatic

**Received:** November 16, 2011
**Revised:** January 5, 2012
**Published:** January 14, 2012

  

interactions. Transfecting pDNA (gWIZ-IL-10) with PEI-TCL-SPION enabled the whole complex to respond profoundly to an applied magnetic force. In addition, direct conjugation of a low-molecular-weight PEI (1200 g/mol) onto commercially available iron oxide coated with gum arabic polysaccharide (Gara) had more PEI on the particle surface than did a physical mixing.[22] This PEI-conjugated Gara was used as a potential vascular drug/gene carrier to brain tumors.

Magnetofection accelerates the sedimentation of gene transfer vectors to the cell surface. The mechanism of magnetofection is thought to be the same as for standard transfection/transduction of gene vectors, except that the MNP is co-internalized with the gene vectors.[23] The MNP based on iron oxide nanoparticles can be degraded under physiological conditions within one month and may be related to ferritin biosynthesis.[24,25] The internalized iron oxide nanoparticles are biotransformed; thus, there would be no safety concern using MNPs as a drug delivery system.

In light of the advantages of using PEI-decorated MNPs as a nonviral gene carrier for magnetofection, the potentials of PEI-PAAIO were examined. The PEI-PAAIO complex was prepared and characterized from an optimized composition of PEI and PAAIO. The weight percent of PEI was measured and used to prepare various N/P ratios between PEI-PAAIO and pDNA. The particle diameters of PEI-PAAIO and its polyplexes with pDNA were characterized using dynamic light scattering (DLS) and a transmission electron microscope (TEM). The iron contents of the internalized PEI-PAAIO/pDNA polyplexes were quantified using an inductively coupled plasma-optical emission spectrometer (ICP-OES) and stained with Prussian blue. The transfection efficiency was tested using pEGFP-C1 and pGL3 plasmids. The internalization of pDNA was visualized using a confocal laser scanning microscope (CLSM). Naked pDNAs were used as a negative control. Branched PEI (MW 25 KDa) was the positive control in the absence of a magnetic field; PolyMag the positive control in the presence of a magnetic field. The superiority of magnetofection using PEI-PAAIO compared with using PolyMag was tested in both HEK 293T and U87 cells.

## 2. EXPERIMENTAL SECTION

**2.1. Materials.** Iron(III) chloride, anhydrous ($FeCl_3$), sodium hydroxide, and poly(acrylic acid) (PAA, $M_w$ 2000 g/mol) was obtained from TCI (Tokyo, Japan). Iron oxide standard solution was acquired from Merck (Darmstadl, Germany). Polyethylenimine (PEI, branched, $M_w$ 25 000 g/mol) was acquired from Polyscience (Warrington, PA, USA). PolyMag was acquired from Chemicell GmbH (Berlin, Germany). *N*-(3-Dimethylaminopropyl)-*N*′-ethylcarbodiimide hydrochloride (EDAC), and 3-(4,5-dimethyl-2-thiazolyl)-2,5-diphenyltetrazolium bromide (MTT) were purchased from Sigma (St. Louis, MO, USA). Potassium hexacyanoferrate (II) trihydrate was from Showa (Tokyo, Japan). Ethidium bromide (EtBr) was purchased from MP Biomedicals (Verona, Italy). Fetal bovine serum (FBS) was acquired from Biological Industries (Beit Haemek, Israel). Agarose, Dulbecco's Modified Eagles Medium (DMEM), Minimal Essential Medium (MEM), penicillin–streptomycin, and Dulbecco's phosphate saline were purchased from Invitrogen-Gibco (Carlsbad, CA, USA). The reporter gene pEGFP-C1 was from Clontech (Palo Alto, CA, USA); pGL3-control and its luciferase assay kit with reporter lysis buffer were purchased from Promega (Madison, WI, USA). A bicinchoninic acid (BCA) protein assay reagent kit was obtained from Pierce Chemical Co. (Rockford, IL, USA). Plasmid DNA (pDNA) was propagated in a chemically competent *E. coli* stain DH5$\alpha$ (GibcoBRL, Gaitherbury, MD, USA), and purified by Viogene Plasmids Maxi kit (Viogene, Sunnyvale, CA, USA). Purity of pDNA was certified by the absorbance ratio at $OD_{260}/OD_{280}$, and by distinctive bands of DNA fragments at corresponding base pairs in gel electrophoresis after restriction enzyme treatments.

**2.2. Synthesis of PAAIO and PEI-Coated PAAIO (PEI-PAAIO).** PAAIO was synthesized by reaction of magnetite nanocrystals with poly(acrylic acid) according to our previous publications.[7,8] PEI-coated PAAIO was prepared by mixing PEI and PAAIO at a stock concentration of 1 mg/mL in double deionized (DD) water. The total volume of 15 mL of PEI and PAAIO prepared at two weight ratios of 1/1 or 1/2 was used for hydrodynamic particle size and zeta potential measurements. The mixture was ultrasonicated (frequency 43K Hz, model D80H, Delta, Taipei, Taiwan) for 5 min. The unbound PEI was removed by placing a permanent magnet (Nd–Fe–B of 6000 G, Taiwan Magnet Co., Taipei, Taiwan) near the test tube and the supernatant solution was carefully withdrawn. The magnetic-attracted PEI-PAAIO complex was redispersed in 15 mL DD water and centrifuged at 6000 rpm for 5 min. The supernatant was combined with the previously withdrawn supernatant for the concentration measurement of unbound PEI. The concentration of PEI was determined by measuring the cuprammonium complex formed between PEI and cupper(II) at 630 nm using a UV–vis spectrophotometer.[21]

**2.3. Characterization of PEI-PAAIO.** PEI-PAAIO was confirmed using a Fourier transform infrared (FTIR) spectrometer. FTIR spectra were performed using a Perkin-Elmer system 2000 spectrometer. Dried samples were ground with KBr powder and pressed into pellets for FTIR measurements. Sixty-four scans were signal-averaged in the range from 4000 to 400 $cm^{-1}$ at a resolution of 4 $cm^{-1}$. Electron spectroscopy for chemical analysis (ESCA) measurements was performed on a ST PHI 5000 Versa Probe (Sliedrecht, Netherlands) spectrometer using a monochromated Al K$\alpha$ X-ray source. The relative atomic concentration of each element at the sample surface was calculated from the peak area using the atomic sensitivity factor specified by the manufacturer. Spectra were recorded over a range of binding energies from 0 to 800 eV with a pass energy of 100 eV for the wide scan survey and a pass energy of 20 eV for high energy resolution spectra for regions of $N_{1s}$. The magnetic properties were measured using a magnetic properties measurement system (MPMS) from Quantum Design (MPMS-XL 7), which utilizes a superconducting quantum interference device (SQUID) magnetometer at fields ranging from −15 to 15 K Oe at 25 °C.

**2.4. Preparation and Characterization of PEI-PAAIO/pDNA Polyplexes.** Since a pDNA concentration in polyplexes was fixed, manipulating the PEI-PAAIO concentration could be used to adjust the N/P ratio between nonviral gene vectors and the pDNA. The pDNA concentration was fixed at 3 $\mu$g/100 $\mu$L in DD water for DNA binding studies and 4 $\mu$g/500 $\mu$L for others. Equal volumes of PEI-PAAIO and pDNA were mixed at N/P ratios from 1 to 30 and immediately vortexed at high speed for 60 s. To verify the stability of polyplexes in solutions with different pH values, PEI-PAAIO/pDNA (N/P = 20) was prepared in DD water of a desired pH value adjusted by using 0.1 M HCl or 0.1 M NaOH . The polyplexes were kept at RT for 30 min for complete complexation before analysis.

*2.4.1. DNA Binding.* DNA binding ability of polyplexes was evaluated using an agarose gel electrophoresis. The polyplexes were prepared at various N/P ratios using the procedure stated above. pDNA (3 $\mu$ g) was complexed with PEI-PAAIO at various N/P ratios. After 0.5 or 4 h standing with or without 10% FBS, the stability of polyplexes was performed by gel electrophoresis with 0.8% agarose containing EtBr (1 $\mu$g/mL). Gels were carried out at 100 V for 50 min and DNA retention was visualized under UV illumination at 365 nm.

*2.4.2. Dynamic Light Scattering (DLS) and Zeta Potential.* The average hydrodynamic diameters and zeta potentials of PAAIO, PEI-PAAIO, and PEI-PAAIO/pDNA were measured using a Zetasizer Nano ZS instrument (Malvern, Worcestershire, UK). Light scattering measurements were carried out with a laser at 633 nm with a 90° scattering angle. The concentration of samples was fixed at 0.1 mg/mL, and the temperature was maintained at 25 °C. Polystyrene nanospheres (Duke Scientific, USA) were used to verify the performance of the instrument (220 ± 6 nm and −50 mV). The


dx.doi.org/10.1021/la204529u | Langmuir 2012, 28, 3542–3552

hydrodynamic particle diameter and zeta potential of each sample was performed in triplicate.

*2.4.3. Transmission Electron Microscopy (TEM).* The sizes and morphologies of polyplexes were visualized using a cryo-TEM (Jeol JEM-1200, Tokyo, Japan). A carbon coated 200 mesh copper specimen grid (Agar Scientific Ltd., Essex, U.K.) was glow-discharged for 1.5 min. One drop of the sample solution was deposited on the grid, and left to air-dry at RT. The sample was then examined using an electron microscope.

**2.5. Cytotoxicity Assay.** HEK 293T cells (human embryonic kidney 293T cell line), and U-87 cells (human glioblastoma cell line) were cultivated at 37 °C under humidified 5% $CO_2$ in DMEM and MEM, supplemented with 10% FBS and 1% penicillin−streptomycin, respectively. The medium was replenished every three days, and cells were subcultured after reaching confluence.

HEK 293T cells were seeded in 12-well tissue culture plates at a density of $1 \times 10^5$ cells per well in DMEM medium containing 10% FBS for 24 h. Cytotoxicity of PEI-PAAIO (5−200 μg/mL) was evaluated by determining the cell viability after 4 h incubation in a serum-free DMEM medium, and 72 h postincubation in the DMEM containing 10% FBS at the same condition for transgene expression. The cytotoxicity of PEI-PAAIO/pDNA was examined at N/P ratios from 1 to 30, where the concentration range of PEI varied from 0.54 to 16.2 μg/mL, and the pDNA concentration was fixed at 4 μg/500 μL. The cytotoxicity of the same polyplex-treated cells was also examined in the presence of a static magnetic field underneath the cells during that 4 h incubation period. An array of 12 Nd−Fe−B disk magnets in the format of a 12-well plate was used. The average magnetic field applied to the center of each well is 3000 ± 400 G. The number of viable cells was determined by estimation of their mitochondrial reductase activity using the tetrazolium-based colorimetric method (MTT conversion test).[26]

**2.6. Transfection Efficiency.** HEK 293T cells were seeded at a density of $1 \times 10^5$/well in 12 well plates and incubated in DMEM containing 10% FBS for 24 h before transfection. When the cells were at 50−70% confluence, the culture medium was replaced with 1 mL of DMEM with or without 10% FBS. Polyplexes at the final volume of 500 μL with 4 μg pEGFP-C1, and various amounts of PEI-PAAIO at N/P ratios from 1 to 30 were prepared. The polyplexes were left to stand for 30 min before addition to the wells. After 4 h incubation with or without a static magnetic field, the medium was replaced with 1 mL of fresh complete medium, and the cells were incubated for 72 h post transfection. The GFP expression was directly visualized under a fluorescence microscope (Zeiss Axiovert 200, Gottingen, Germany).

For the luciferase assay, the procedures as stated above were repeated to determine the transfection efficiency of pGL3 plasmid in HEK 293T cells cultured in DMEM, and U-87 cells cultured in MEM. The transfection efficiency of polyplexes was compared with naked DNA (as a negative control), and PEI/DNA polyplex at an N/P ratio of 10 when an external magnetic field is absent, and PolyMag when an external magnetic field is present as a positive control. The optimized conditions for magnetofection of PolyMag were adopted from the company protocol (4 μL of PolyMag and 4 μg of pDNA). To quantify the luciferase expression, transfected cells were rinsed gently with 1 mL of 0.1 M PBS (twice), and then added to 200 μL/well of lysis buffer (0.1 M Tris-HCl, 2 mM EDTA, and 0.1% Triton X-100, pH 7.8) and let stand overnight at −20 °C. Next day, each cell lysate was warmed to RT, and then transferred into a 1.5 mL microcentrifuge tube for centrifugation at 15 000 rpm for 30 min. The luciferase activity was monitored using a TopCount NXT microplate scintillation and luminescence counter (Perkin-Elmer, NJ, USA) after mixing 50 μL/well of supernatant with 50 μL/well of luciferase assay reagent (Promega, Madison, WI, USA). The total protein content of the cell lysate was examined using a BCA protein assay kit, and was performed according to the protocols provided by the manufacturer (Pierce Rockford, IL, USA).

**2.7. Cellular Uptake.** The internalized iron amount of PEI-PAAIO followed the experiment described in section 2.6 was quantified using an inductively coupled plasma-optical emission spectrometer (ICP-OES, Optima 7000DV, Perkin-Elmer, Boston, MA, USA). The count of $2 \times 10^5$ cells from each sample was analyzed for iron content. The protein content of the half cell lysate was examined using a BCA protein assay kit. The other half cell lysate was dissolved in 37% HCl and incubated at 70 °C for 1 h. The samples were diluted to a final volume of 3 mL for analysis. The iron content of samples were calculated based on an $Fe(NO_3)_3$ calibration curve.

The internalized PEI-PAAIO nanoparticles within HEK 293T cells were directly visualized using Prussian blue staining of iron. After 4 h incubation with PEI-PAAIO as previously mentioned, the cells were washed with 0.1 M PBS (thrice), fixed with 3.7% formaldehyde (1 mL/well) for 10 min, and washed again with PBS (thrice). Prussian blue solution was prepared by mixing 10 mL of 2% potassium hexacyanoferrate (II) trihydrate solution, and 5 mL of 2% HCl. The Prussian blue solution of 1 mL/well was added and incubated with the cells for 30 min. The internalized $Fe^{3+}$ ions of PAAIO turn to bright blue pigment when reacted with the ferrocyanide ions. This blue color is visualized using an optical microscope (Nikon, TE 2000U, Tokyo, Japan).

**2.8. Cell Internalization by CLSM.** The intracellular delivery of pDNA was observed using CLSM.[27] U87 cells were seeded at a density of $1.5 \times 10^5$ cells/well in 12 well plates containing one glass coverslip/well in MEM supplemented with 10% FBS, and incubated for 24 h. The polyplex was prepared at an N/P ratio of 20 between PEI-PAAIO and Cy5-labeled pGL3-control plasmid. The pGL3-control plasmid was labeled with Cy5 using a Mirus *Lebal* IT nucleic acid labeling Kit (MIR-3700, Mirus, Pittsburgh, PA, USA) following the protocol supplied by the manufacture. Briefly, 20 μg pDNA were incubated with the Mirus Cy-5 reagent for 1 h and purified with ethanol precipitation method. The Cy5-labeled pDNA was resuspended into 20 μL DD water and stored at −20 °C in the dark for future use.

The U87 cells were exposed to the polyplex for 4 h at 37 °C with or without exposure to a magnetic field. After incubation, the medium containing the polyplex was removed. The coverslips were washed gently with 1 mL of 0.1 M PBS (twice), and then treated with 100 nM Lysotracker (DND-26, Invitrogene, Carlsbad, CA, USA) for 2 h at 37 °C. Next, the coverslips were removed, washed gently with 1 mL of 0.1 M PBS (5 times), placed in a new empty well, and treated with 1 mL of 3.7% paraformaldehyde in 0.1 M PBS for 15 min to fix the cells. The cells were treated with 1 mL/well of 0.1% Triton X-100, and incubated for 10 min. After three washings with PBS, the cells were incubated at 37 °C with 0.5 mL/well of DAPI for 10 min. After DAPI staining, the cells on the coverslips were washed three times with PBS, and mounted on glass slides by fluorescent mounting medium. Olympus Fv 1000 CLSM (Tokyo, Japan) was used for cell imaging.

**2.9. Statistical Methods.** Means, SD, and SE of the data were calculated. Differences between the experimental groups and the control groups were tested using Student's-Newman-Keuls' test and $P < 0.05$ was considered significant.

## 3. RESULTS

**3.1. Characterization of PEI-PAAIO.** To obtain a stable PEI-PAAIO complex, various weight ratios between PAAIO and PEI were tested at three pH values: 2.0, 6.8, and 11. The weight ratios of 1:1 and 2:1 between PAAIO and PEI were chosen for hydrodynamic diameter and zeta potential measurements since no turbidity occurred when mixing the two solutions. PAAIO had an average hydrodynamic diameter of 30 nm and a negative zeta potential of −25 mV (Supporting Information Figure S1). At pH 6.8, both PEI-PAAIO complexes showed similar zeta potentials of +22 mV, but the complex with the weight ratio of 2:1 had an average hydrodynamic diameter of about 77 nm, which was smaller than that prepared from 1:1 (∼101 nm). The hydrodynamic diameter at the weight ratio of 2:1 between PAAIO and PEI was stable in DD water within 14 days of testing (Supporting Information Figure S2). Thus, MNP prepared at this weight ratio was used for later studies. The positive zeta potential of the complexes implied the

successful decoration of PEI on PAAIO. The spectroscopic evidence of PEI decoration could be seen in FTIR (Figure 1A),

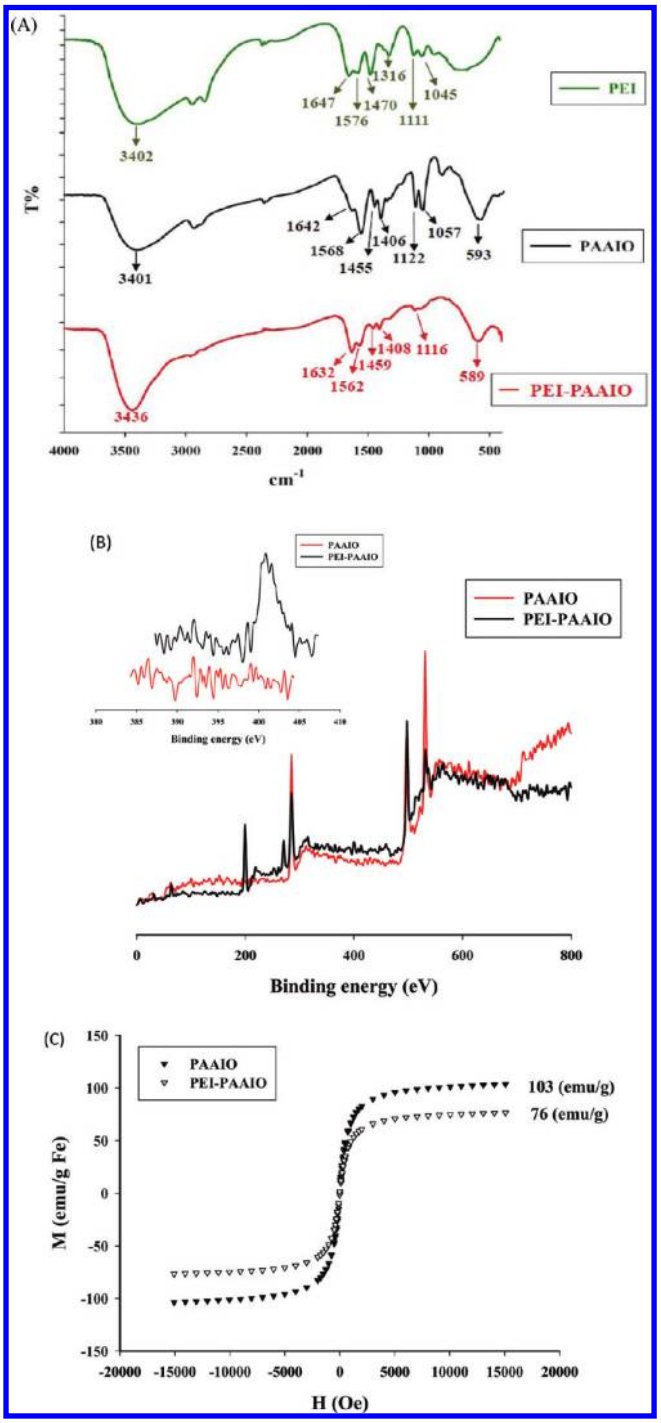


**Figure 1.** Spectroscopic evidence and superparamagnetism of PEI-PAAIO: (A) FTIR spectra; (B) ESCA spectra; (C) SQUID magnetization curves.

where PAAIO showed three characteristic stretching bands at 1568, 1455, and 1406 $cm^{-1}$, and PEI appeared at 1647, 1576, and 1470 $cm^{-1}$. After forming the complex between PAAIO and PEI, the primary amine stretching of PEI at 1647 $cm^{-1}$ shifted to 1632 $cm^{-1}$, and the asymmetric carboxylate peak at 1568 $cm^{-1}$ shifted to 1562 $cm^{-1}$ because of the electrostatic interactions. Moreover, the peak intensity of the carboxylate stretching of PAAIO at 1562 $cm^{-1}$ decreased because of a surface coating of PEI. Additional evidence of PEI decorated on PAAIO was observed using an ESCA where the binding energies of atoms $C_{1s}$, $N_{1s}$, and $O_{1s}$ appeared at 283, 400, and 530 eV. The atom percentage of N was undetectable in PAAIO, but a value of 4.7% was measured in PEI-PAAIO (Figure 1B). The saturation magnetization ($M_s$) value of PEI-PAAIO was 76 emu/g Fe and 103 emu/g Fe for PAAIO (Figure 1C). As expected, the $M_s$ decreased after PEI was coated on PAAIO. The PEI-PAAIO still remained highly superparamagnetic at RT and showed negligible hysteresis. PAAIO had a residual magnetization ($M_r$) of 1.8 emu/g Fe and coercivity (Hc) of 13.6 Oe, and the PEI-PAAIO had a slight change in $M_r$ (1.6 emu/g Fe) and Hc (12.9 Oe).

The concentration of PEI in PEI-PAAIO was determined by measuring the cuprammonium complex formed between PEI and copper(II) at 630 nm using a UV−vis spectrophotometer.[21] The value of 0.135 ± 0.03 mg/mL was obtained based on a calibration curve of PEI with a linear regression value of 0.9949. The theoretical molecular weight of PAAIO was 2232 g/mol, and that of branched PEI was 25 000 g/mol. The calculated molar percent of PEI in PEI-PAAIO was 1.37 mol %, which was used to prepare various N/P ratios between PEI-PAAIO and pDNA in this study.

**3.2. Characterizing PEI-PAAIO/pDNA Polyplexes.** By changing PEI-PAAIO weight and keeping pDNA weight as a constant, various N/P ratios of PEI-PAAIO/pDNA polyplexes were prepared (Scheme 1). The binding ability between PEI-PAAIO and pDNA was studied using an agarose gel electrophoresis retardation assay. To verify the protection of pDNA against serum digestion, the electrophoretic mobility analysis of the PEI-PAAIO/pDNA polyplexes was tested after it had been left standing for 0.5 or 4 h in 10% FBS at RT. The pDNA was well-complexed at an N/P ratio of >5. The pDNA was stable at 0.5 h in polyplexes with and without FBS (Figure 2A), but it was completely degraded after 4 h of incubation with 10% FBS (Figure 2B). After 4 h standing in the medium without 10% FBS, we could clearly observe the pDNA exposure at the N/P = 5 polyplex. Nevertheless, FBS did not affect the pDNA property when the N/P ratio of PEI-PAAIO/pDNA was >7 (Figure 2B). At an N/P ratio of >15, pDNA was well-protected with or without FBS. With this test result, we ensured the stability of pDNA complexed within PEI-PAAIO if we prepared the PEI-PAAIO/pDNA at an N/P ratio of ≥7.

The hydrodynamic diameters of PAAIO and PEI-PAAIO were approximately 30 and 77 nm measured by DLS. After forming PEI-PAAIO/pDNA polyplexes, the average hydrodynamic diameter increased to 150 nm at N/P ratios of 3 and 5, maximized at 7 (250 nm), and decreased dramatically to <100 nm when the N/P ratio was >9 (Table 1). The surface charge of PAAIO was −25 mV and turned to a positive value of 22 mV following PEI decoration. This positive value of zeta potential also indicated the successful coating of PEI onto PAAIO. When the amount of PEI-PAAIO was low, the formed PEI-PAAIO/pDNA polyplexes showed negative surface charges (at the N/P ratios of 3 and 5). At an N/P ratio of 7, the zeta potential of the polyplex fluctuated seriously between positive and negative values, which is attributable to a charge balance between positive PEI-PAAIO and negative pDNA at this N/P ratio. An increase in an N/P ratio of >7 resulted in an increase in positive zeta potential and a decrease in the hydrodynamic diameter of polyplexes. The polyplex at an N/P ratio of 30 had a zeta potential close to PEI-PAAIO (22 mV) and a small


dx.doi.org/10.1021/la204529u | Langmuir 2012, 28, 3542−3552

**Scheme 1. Preparation of PEI-PAAIO/pDNA Magnetoplexes**

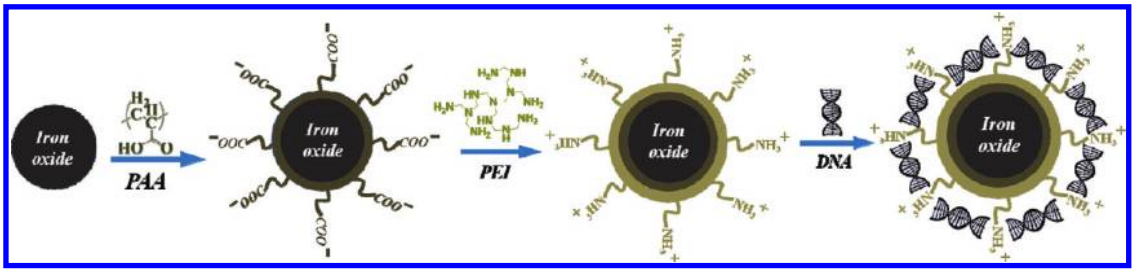


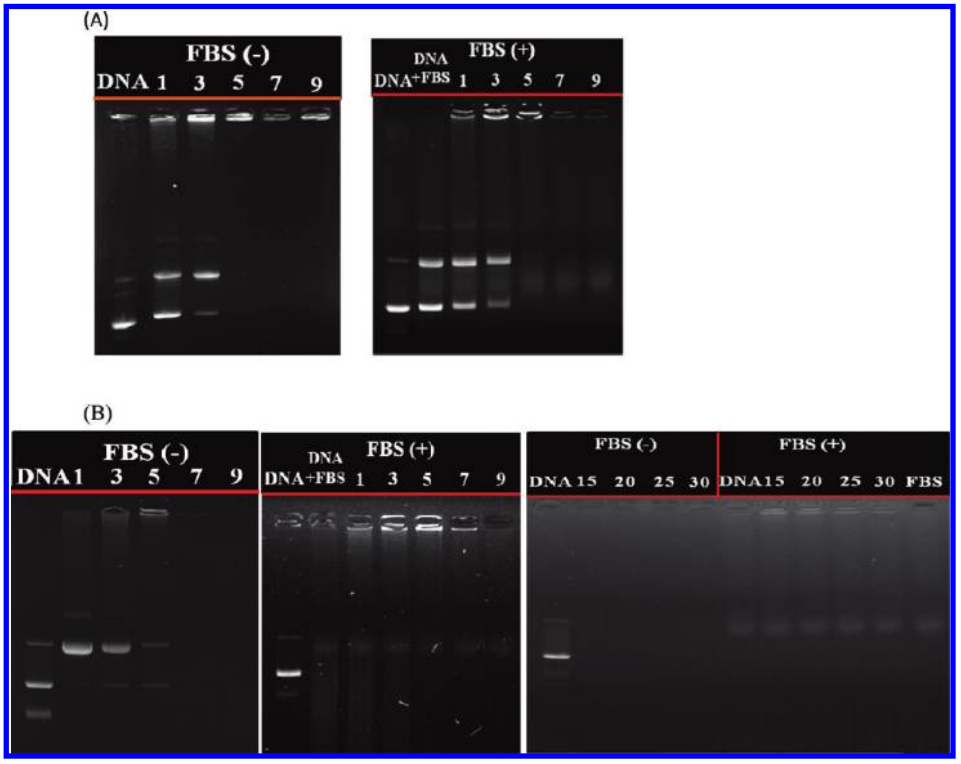


**Figure 2.** Agarose gel electrophoresis to test pDNA retention in PEI-PAAIO/pDNA magnetoplexes prepared at various N/P ratios after 0.5 h (A) and 4 h standing (B) with 10% FBS(+) or without FBS(−) medium. The numerals at the top of each graph indicate the N/P ratio between PEI-PAAIO and pDNA.

**Table 1. Hydrodynamic Diameters and Zeta-Potentials of PEI-PAAIO/pDNA Polyplexes at Various N/P Ratios[a]**

| N/P | diameter ($D_h$, nm) | zeta (mV) | PDI | $K_{cp}$ |
|---|---|---|---|---|
| 3 | 158.4 + 39.0 | −24.2 + 0.9 | 0.23 + 0.04 | 185.8 + 13.5 |
| 5 | 167.0 + 12.9 | −19.4 + 2.0 | 0.19 + 0.01 | 307.7 + 73.9 |
| 7 | 266.5 + 66.0 | −2.4 + 16.3 | 0.63 + 0.14 | 346.4 + 122.1 |
| 9 | 83.1 + 0.9 | 17.4 + 4.1 | 0.25 + 0.08 | 275.2 + 68.2 |
| 15 | 65.5 + 16.1 | 17.7 + 2.0 | 0.20 + 0.04 | 133.7 + 20.1 |
| 20 | 60.8 + 11.0 | 18.2 + 2.0 | 0.26 + 0.02 | 140.8 + 7.2 |
| 25 | 56.2 + 9.3 | 21.3 + 2.4 | 0.26 + 0.04 | 141.4 + 10.4 |
| 30 | 53.9 + 9.8 | 21.9 + 1.8 | 0.28 + 0.05 | 156.3 + 6.1 |

[a]The concentration of samples was 0.1 mg/mL and the temperature was 25 °C. The data represent means + SD of an experiment performed in triplicate. PDI: Polydispersity index; $K_{cp}$: Light count rate.

hydrodynamic diameter (54 nm). The hydrodynamic diameters and zeta potentials of PEI-PAAIO/pDNA at N/P ratios ranging from 15 to 30 and standing for 4 h in DD water containing 10% FBS were also measured. The hydrodynamic diameter increased from approximately 60 to 90 nm and the zeta potential decreased from approximately +20 to −10 mV because of the surface coating of FBS (Supporting Information Figure S3). The stability of the polyplexes in different pH solutions was also tested in the PEI-PAAIO/pDNA at an N/P ratio of 20. The results showed that the hydrodynamic diameter was stable when the pH ranged from 5 to 7 (61−72 nm) but doubled (135 nm) when the pH was 8 (Supporting Information Table S1).

In Figure 3A, the TEM morphological image of PAAIO showed uniform particle distribution; the average particle diameter was 8.62 ± 1.82 nm. PAAIO was stable after 9 months in DD water.[8] Stable particle size and distribution after PEI decoration was seen in Figure 3B. The average particle diameter of PEI-PAAIO slightly increased to 9.31 ± 3.21 nm. The smaller particle diameters than those measured by DLS are because the samples prepared for TEM measurement are in a dry state. When the polyplexes were prepared at N/P ratios of 15, 20, 25, and 30 between PEI-PAAIO and pDNA, all appeared as clusters with evenly distributed small dots. The measured cluster particle diameters are 103.6 ± 16.5, 105.4 ± 19.9, 128.8 ± 14.4, and 95.8 ± 11.2 nm, respectively, for the N/


dx.doi.org/10.1021/la204529u | Langmuir 2012, 28, 3542−3552

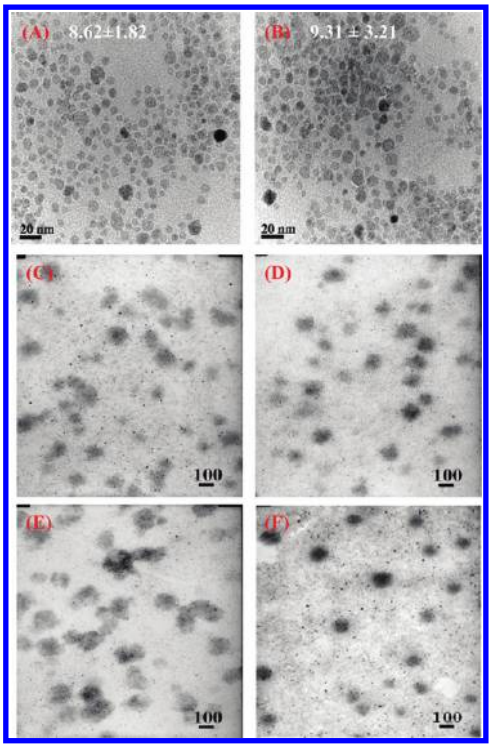


**Figure 3.** TEM images of (A) PAAIO, (B) PEI-PAAIO, and PEI-PAAIO/pDNA polyplexes prepared as stated in the text at N/P ratios of (C) 15, (D) 20, (E) 25, and (F) 30.

P ratios of 15, 20, 25, and 30 (Figure 3C–F). TEM shows no clear correlation between particle size and N/P ratio.

**3.3. Cytotoxicity.** The cell viability of PEI-PAAIO was tested using an MTT assay with HEK 293T cells 72 h after they had been incubated at 37 °C for 4 h.[25] PEI-PAAIO showed negligible cytotoxicity in all tested concentrations (Figure 4A). PEI-PAAIO/pDNA polyplexes with N/P ratios ranging from 1 to 30 showed minimal cytotoxicity (Figure 4B). The cell viabilities at any N/P ratios were all >80% because the PEI concentration of PEI-PAAIO/pDNA used to make the highest N/P ratio of 30 was 16.2 $\mu$g/mL, which was minimal toxic to HEK 293T cells. The cells exposed to pure PEI at concentrations of 10 and 20 $\mu$g/mL showed 92% and 65% cell viabilities, respectively. The lower cytotoxicity of the polyplexes compared with the two positive control groups, PEI and PolyMag, might be attributable to the lower PEI content used in the PEI-PAAIO/pDNA preparation. The cell viability was not affected by applying an external magnetic field underneath the cells.

**3.4. *In Vitro* Gene Transfection.** After determining that the PEI-PAAIO showed good complexation and minimal cytotoxicity with pDNA, we tested *in vitro* magnetofection activity in the presence and absence of FBS. The magnetic field was generated by placing an array of 12 Nd–Fe–B disk magnets in the format of a 12-well plate underneath a 12-well plate containing cells. The resultant vector dose of the individual magnet was concentrated at the center of an individual well; the magnetic field was 3000 ± 400 G. The cells were incubated with PEI-PAAIO/pDNA polyplexes at 37 °C for 4 h with or without 10% FBS. The cells were postincubated for another 72 h to transport pDNA to the nuclei for transfection. Two plasmid DNAs, pEGFP-C1 (for fluorescence measurement) and pGL3-control (for luminescence measurement), were used to test the transfection efficiency of PEI-PAAIO as a nonviral gene carrier.

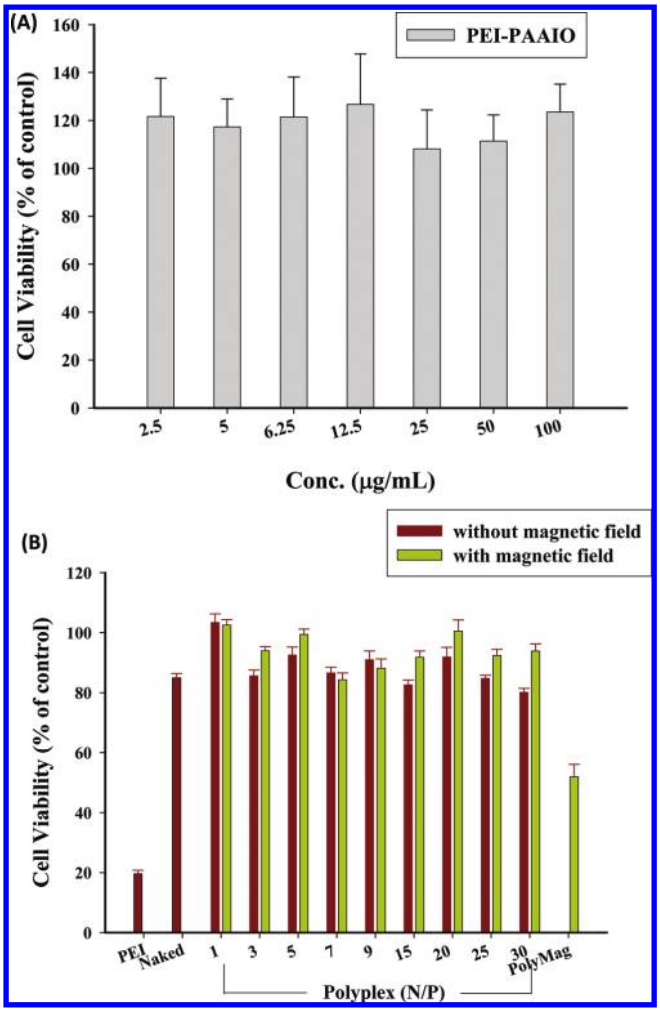


**Figure 4.** MTT assay of the cytotoxicity of PEI-PAAIO and its polyplexes to HEK 293T cells. (A) PEI-PAAIO as a function of PEI-PAAIO concentrations and (B) PEI-PAAIO/pDNA polyplexes at different N/P ratios with and without a magnetic field.

The relative green fluorescence expression, a measure of transfection efficiency, from pEGFP-C1 was traced using a fluorescence microscope without 10% FBS [FBS(−)] (Figure 5A) and Figure 5B with 10% FBS [FBS(+)]. The green fluorescence expression of the polyplexes was significantly lower than that of the PEI/pDNA in FBS(−) medium (Figure 5A). The green fluorescence expression was clearly observed when the PEI-PAAIO/pEGFP ratio increased to 15; it peaked at 20 with a magnetic field and 25 without a magnetic field.

pEGFP expression of PEI/pDNA was significantly lower in FBS(+) medium. However, the expression of PEI-PAAIO/pEGFP significantly increased at N/P ratios >15 (Figure 5B); the relative green fluorescence intensity increased more than 7 times if a magnetic force was applied. The green fluorescence images are also shown in the panels below Figure 5A,B to demonstrate how much stronger gene expression was with (M(+)) than without (M(−)) magnetic force in FBS(+) medium than in FBS(−) medium.

A quantitative comparison of transfection ability of the polyplexes with PEI/pDNA and PolyMag/pDNA with and without 10% FBS was also done by measuring luciferase gene


dx.doi.org/10.1021/la204529u | *Langmuir* 2012, 28, 3542–3552

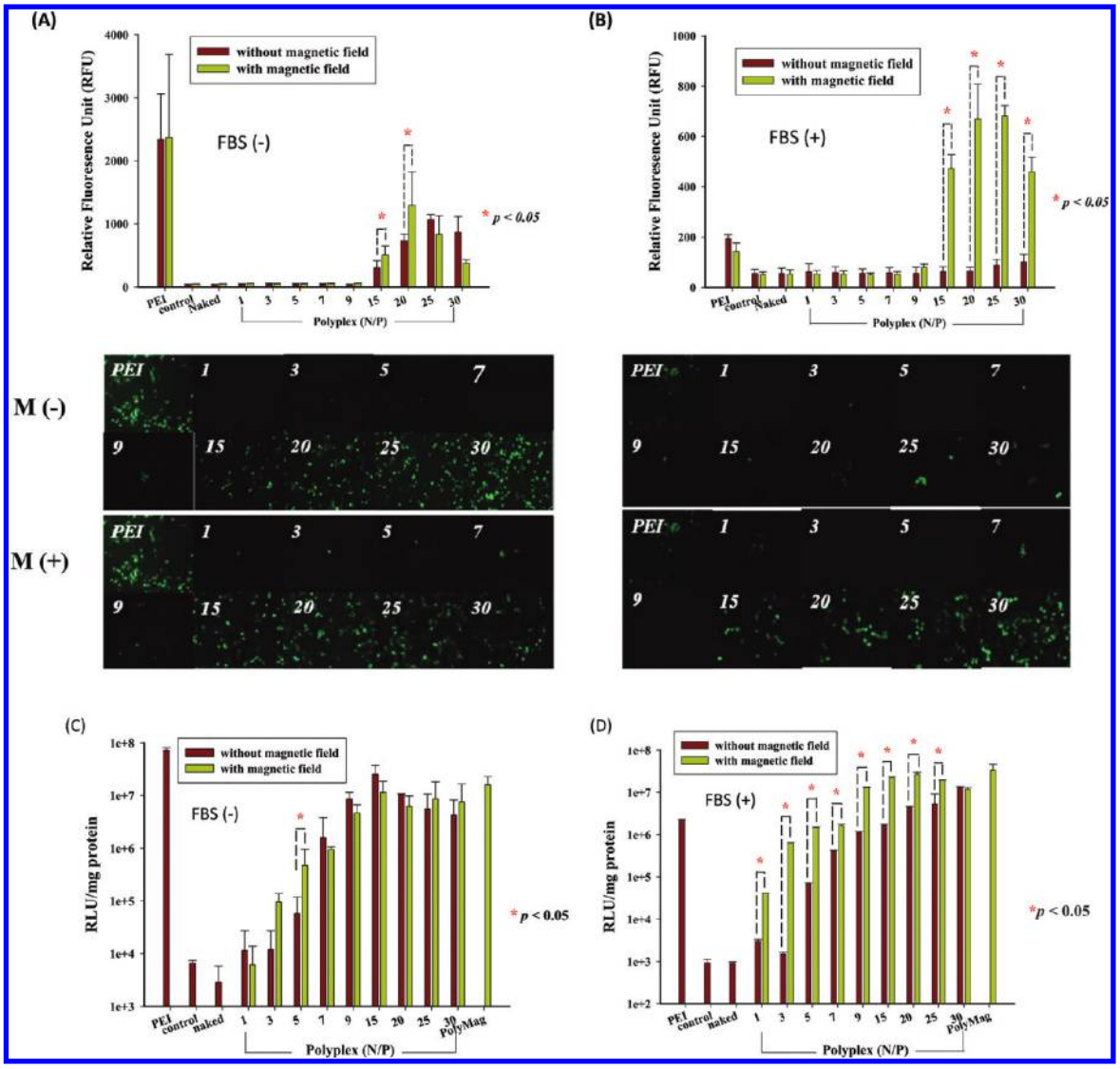


**Figure 5.** Gene expression in HEK 293T cells as a function of polyplex compositions. Fluorescence intensity and optical images of pEGFP-C1 expression in (A) FBS(−) medium and in (B) 10% FBS(+) medium. Luciferase activity normalized with protein amounts in (C) FBS(−) medium and in (D) 10% FBS(+) medium in 293T cells exposed to PEI-PAAIO/pDNA polyplexes with and without a magnetic field.

expression of pGL3-control plasmid (Figure 5C,D). The result was consistent with the findings in Figure 5A,B. The transfection efficiency of PEI-PAAIO/pDNA was competitive with that of a commercial product, PolyMag/pDNA.

**3.5. Cellular Uptake.** The internalization of PEI-PAAIO in HEK 293T cells was directly stained with Prussian blue. The internalized $Fe^{3+}$ ions of PAAIO turned to bright blue pigment when reacting with the ferrocyanide ions. This blue color was visualized using an optical microscope. There was no discernible difference between cells with and without an imposed magnetic field in FBS(−) medium. In FBS(+) medium, cells became increasingly bluer with an increasing N/P ratio between PEI-PAAIO and pDNA with an imposed magnetic field (Figure 6B). Magnetic polyplexes in serum media increase the gravitational sedimentation and magnetic attraction of the gene vector onto the cells when a magnetic field is placed underneath,[28] and our polyplexes clearly showed a greater cellular internalization when assisted by a magnetic field.

The quantity of iron normalized to total cell population was determined using an ICP-OES. The amount of iron internalized within the cells showed no consistent correlation with an increasing N/P ratio when there was no magnetic field, but the amount was dose-dependent when there was a magnetic field (Figure 6C) in FBS(−) medium; approximately twice as much iron was internalized in FBS(+) medium when there was a magnetic field (Figure 6D).

To evaluate the transfection efficiency of PEI-PAAIO/pDNA for its *in vivo* applicability to brain tumors, we used human glioblastoma U-87 cells. The transfection efficiency consistently increased at most N/P ratios, with and without a magnetic field, with an increase in the N/P ratio in FBS(−) medium (Figure 7A). Although the transfection efficiency decreased in FBS(+) medium without a magnetic field, it was significantly augmented when there was a magnetic field (Figure 7B). ICP-OES analysis showed similar results (Figure 7C,D).

To directly visualize the pDNA inside U87 cells, we labeled pDNA with a fluorescent Cy5 dye and traced the Cy5-labeled pDNA using CLSM. The nuclei were stained with DAPI in blue and the endolysosomes with Lysotracker in green. Cellular uptake of pDNA is shown in red fluorescence, which is conspicuously absent in the micrographs of cells without a


dx.doi.org/10.1021/la204529u | *Langmuir* 2012, 28, 3542−3552

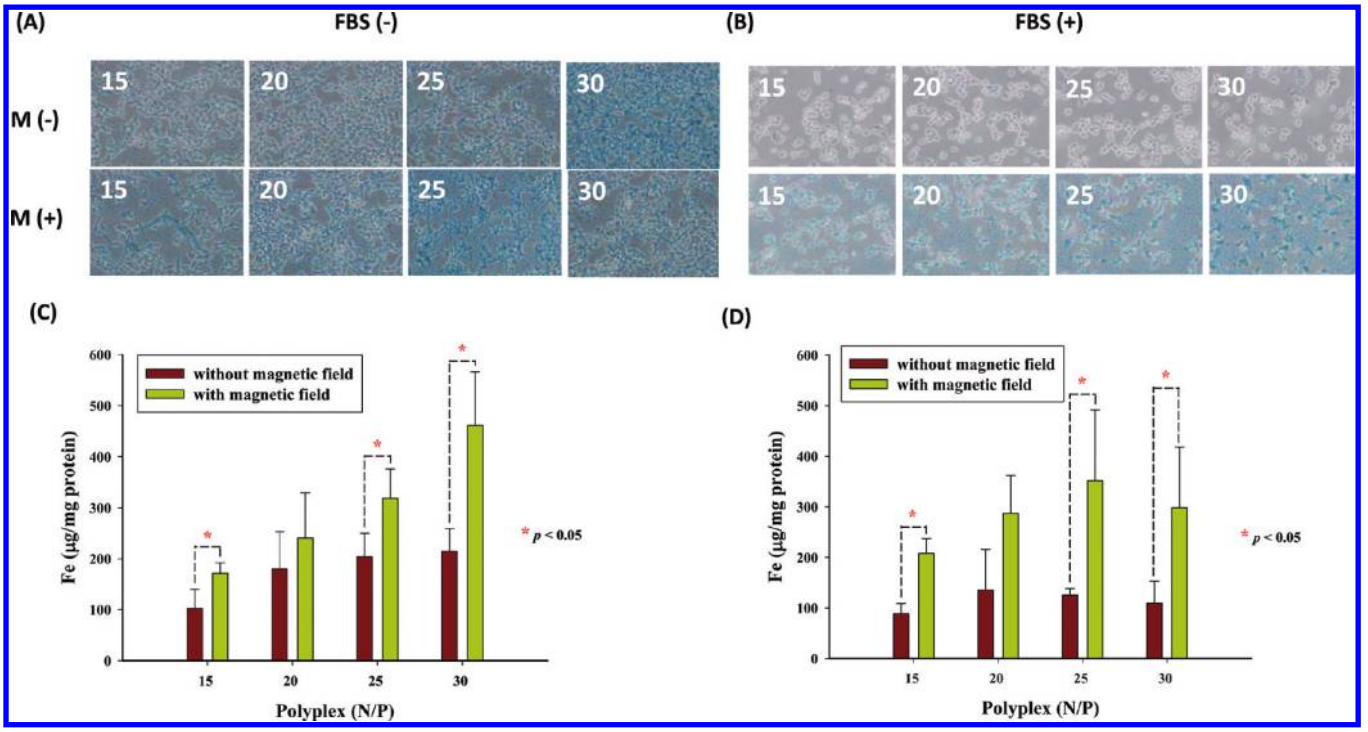


**Figure 6.** Internalization of iron oxide particles uptaken by HEK 293T cells at various N/P ratios of PEI-PAAIO/pDNA. The internalized PEI-PAAIO was directly visualized using Prussian blue staining in (A) FBS(−) medium and in (B) 10% FBS (+) medium. The internalized iron uptake by 293T cells quantified using ICP-OES in (C) FBS(−) medium and in (D) 10% FBS(+) medium.

magnetic field (Figure 8A) but easily visible in those of cells with a magnetic field (Figure 8B(c,d)). Because the internalized Cy5-labeled pDNA (red) and the stained endolysosomes (green) did not overlay, the delivery of the pDNA to the perinuclear region of U87 cells was confirmed.

## 4. DISCUSSION

MNPs composed of an iron oxide core and a polymeric shell are promising carriers for the targeted delivery of therapeutic payloads.[29] MNPs in the form of superparamagnetic iron oxide (SPIO) are interesting because they can be used as a magnetic resonance imaging (MRI) contrast agent.[30] Iron oxide particles will degrade under physiological conditions within one month, which may be related to ferritin biosynthesis.[24,25] Therefore, when used as vehicles for nanomedicine, these MNPs will be nontoxic.

Although PEI is a gold standard nonviral gene delivery vector, the clinical applications are limited because of its high cytotoxicity. To overcome this hurdle, we coated PEI on the PAAIO surface to reduce the amount of PEI used as a gene vector. After being coated with PEI, the PEI-PAAIO could be used not only as a nonviral gene vector for increased gene delivery rate by magnetofection, but also as an MRI contrast agent[7] because of its high superparamagnetism (103 emu/g Fe).

The PEI wt % was controlled at 33.3 wt % in feed. After the coating had been applied, the PEI content of a PEI-PAAIO MNP was 13.5 wt %. This implied that increasing the PEI coating concentration to 50 wt % in feed might not simultaneously increase the PEI content in PEI-PAAIO. Moreover, the PEI-PAAIO prepared from the weight ratio of 1:2 between PEI and PAAIO had the smallest hydrodynamic diameter of 77 nm and a positive zeta potential of 22 mV. The successful coating of PEI onto the PAAIO surface was evidenced by FTIR, ESCA, and zeta potential measurements. Thus, the optimized conditions to produce a stable PEI-PAAIO complex were found to be pH 6.8 and a weight ratio of 2:1 between PAAIO and PEI.

The PEI concentration of a PEI-PAAIO MNP was 0.135 ± 0.03 mg/mL, which was relevant to the 5.4 nmol PEI per mg of PEI-PAAIO nanoparticles. This value was less than that reported in the literature.[22] A low molecular weight PEI (1200 g/mol) was decorated on Gara using a chemical conjugation; a value of approximately 15.5 nmol of PEI per mg of nanoparticles was obtained.[22] The lower PEI content in PEI-PAAIO might be because of weaker electrostatic interactions between PEI and PAAIO compared with a chemical conjugation or because of a higher molecular weight of PEI (25 000 g/mol) used in this study, leading to increase the structural hindrance in forming electrostatic interactions.

The presence of proteins under physiological conditions may accelerate pDNA dissociation in the bloodstream.[28] To verify this concern, the stability of pDNA was analyzed using agarose gel electrophoresis. PEI-PAAIO/pDNA polyplexes had been prepared and allowed to stand with and without 10% FBS for 4 h; the pDNA was well-protected at an N/P ratio ≥7.

The TEM images in Figure 3 showed uniformly small dots distributed within big clusters. These small dots were suspected to be pDNA-uncomplexed PEI-PAAIO MNPs, PAAIO MNPs, or other MNPs. Uncomplexed MNPs have increased transgene expression in PEI-MNP gene delivery systems,[20,28] but the role of uncomplexed MNPs in improving gene transfection efficiency is unknown.

The PEI-PAAIO/pDNA magnetoplexes formed compact particles with an increasing N/P ratio, and the sizes were larger than those reported in the literature.[4,21,28] *In situ* preparation of PEI-based MNPs using two PEI molecular weights of 10 and 160 KDa showed an average particle diameter of 3 nm (TEM


dx.doi.org/10.1021/la204529u | *Langmuir* 2012, 28, 3542−3552

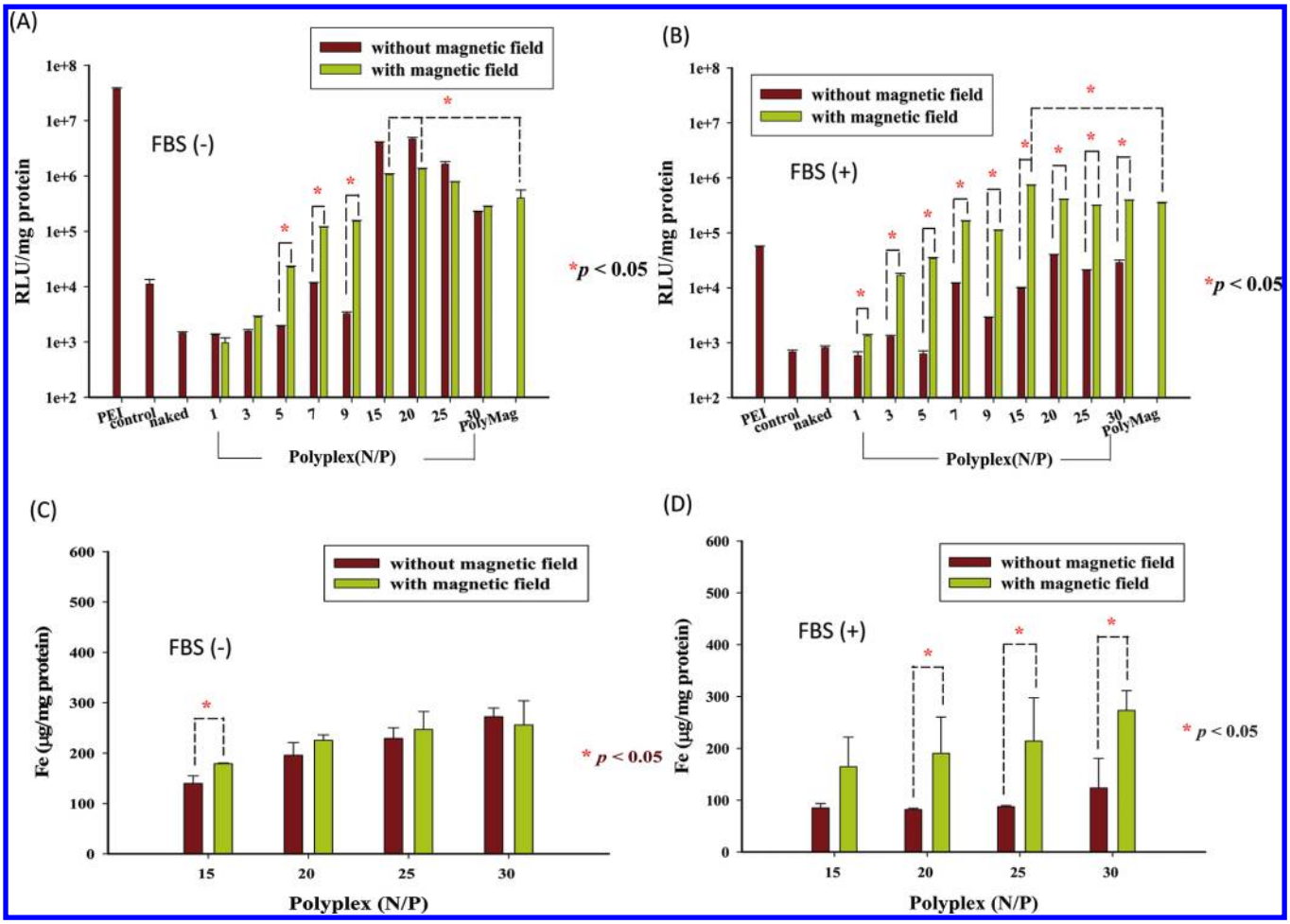


**Figure 7.** Gene expression and iron uptake in U87 cells as a function of polyplex compositions. Luciferase activity in U87 cells exposed to PEI-PAAIO/pDNA polyplexes in (A) FBS(−) medium and in (B) 10% FBS(+) medium with and without a magnetic field. The U87 cell-internalized iron amount quantified using ICP-OES in (C) FBS(−) medium and in (D) 10% FBS(+) medium.

measurements).[4] There are two explanations for the smaller particle size: first, the restriction of MNPs to the interiors of PEI, and, second, the crystal growth and reorganization became relatively slow compared with iron oxide nanoparticles synthesized by small stabilizers. Chemically conjugated PEI onto MNP followed by association with pDNA formed cloud-like particles with an average diameter of 50 nm (TEM measurements).[21] Another study[28] reported a similar polyplex preparation to ours; the particle size was approximately 112 nm, but the particles aggregated in DMEM. The magnetite core diameter of PEI-Mag2 was 9 nm, and the hydrodynamic diameter of whole nanoparticles was 63 ± 36 nm, but there was no data on the relevant particle diameter after forming the magnetoplex between PEI-Mag2 and pDNA.[20] A larger hydrodynamic particle size of 225 nm was reported[19] for a low molecular weight PEI-coated Gara system.

The size discrepancy between PEI-coated MNPs was primarily because of the amount and molecular weight of the PEI used. Nevertheless, the duration time and the vortex for complex formation could also be a determining factor. The larger MNPs (375 nm in diameter) had higher transfection rates than the smaller (180 or 210 nm in diameter) MNPs.[31] Another concern about particle size is the pharmacokinetics of *in vivo* delivery. Particles had better be 10−200 nm in diameter to escape renal clearance (<10 nm) and sequestration by the reticuloendothelial system (RES) of the spleen and liver (>200 nm).[32] Thus, we tried to restrict the PEI-PAAIO/pDNA particle sizes to approximately 100 nm, not only to optimize a good transfection rate, but also to prevent their sequestration by the RES.

The cytotoxicity of gene vectors is always a major concern for their clinical use.[33,34] In general, the branched PEI of MW 25 KDa showed high cytotoxicity in cells when the concentration was higher than 50 μg/mL.[35−37] The higher cell viability of PEI-PAAIO may be attributable to the lower PEI content (only 13.5 wt % in PEI-PAAIO). Based on our cytotoxicity study, PEI-PAAIO seems superior to pure PEI or PolyMag as a nonviral gene vector. Constructed cationic mesoporous silica nanoparticles (MSNP) modified with PEI at a proper size increase intracellular delivery of nucleic acids with minimal or no cytotoxicity.[38] We expect that PEI-PAAIO will be as efficient and safe a gene carrier as MSNP-modified PEI.

In comparison, gene expression was greater when FBS was absent. However, under physiological conditions, many proteins interfere with the stability of pDNA/vector complexes, which reduces gene transfection efficiency. The green fluorescence intensity of PEI/pDNA was reduced dramatically when 10% FBS was added into the cell culture medium. This was because of the competition between FBS and pDNA with PEI, which reduces the pDNA concentration in the polyplexes.[39,40] In addition, the FBS adsorption on the PEI/pDNA surface also inhibits transgene expression.[41]


dx.doi.org/10.1021/la204529u | *Langmuir* 2012, 28, 3542−3552

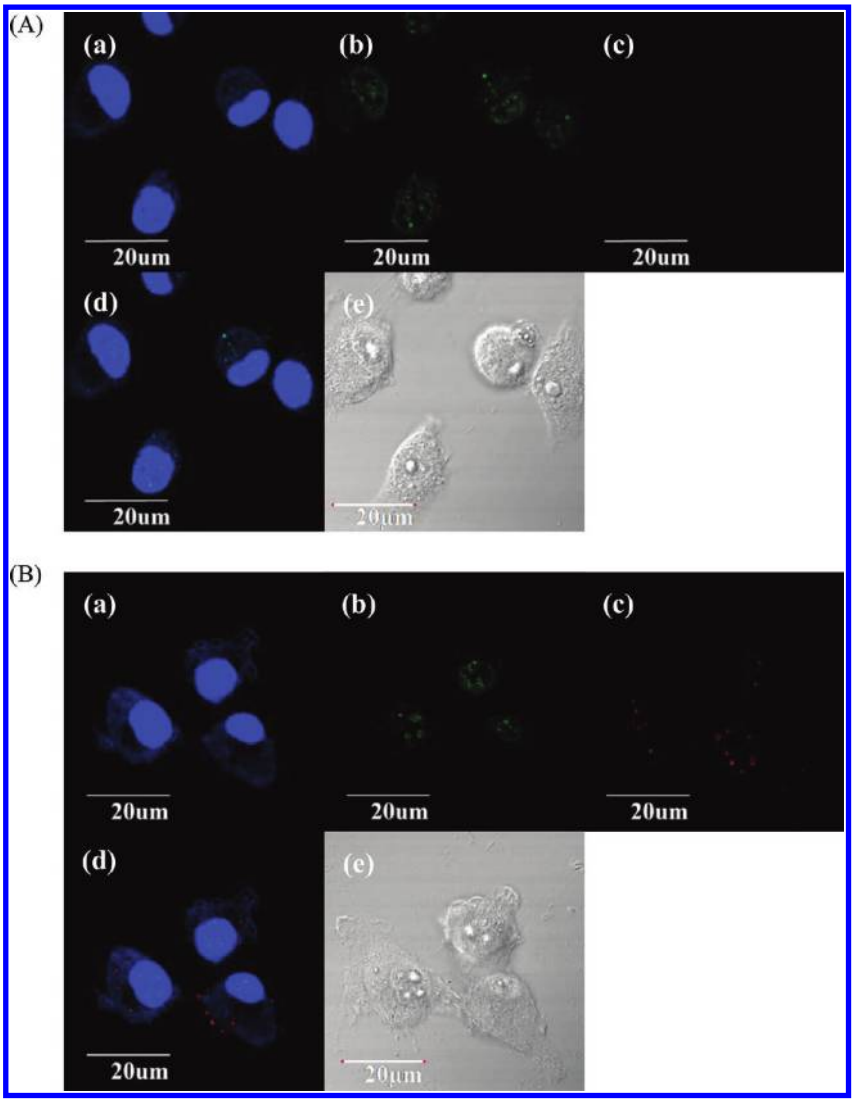


**Figure 8.** CLSM images of U87 cells exposed to the Cy5-labeled pDNA (1 μg/well) polyplex of PEI-PAAIO/pDNA at an N/P ratio of 20 in 10% FBS(+) medium for 4 h at 37 °C without (A) and with (B) a magnetic field. (a) Blue: nuclei (DAPI), (b) green: Lysotracker, (c) red: Cy5-labeled pGL3 plasmid, (d) merged (b) and (c), (e) DIC of the cells.

Screening of transfection efficiencies under varied N/P ratios between PEI-PAAIO and pEGFP with FBS revealed a large and significant increase in the magnetic effect at an N/P ratio of ≥15. The rapid internalization of the polyplexes with the high N/P ratios into the cells prevented pDNA destabilization from FBS interference during that incubation period. Nevertheless, a gene transfection study in U87 cells showed a result opposite that in 293T cells in FBS(−) medium. At an N/P ratio of ≥15, the PEI-PAAIO/pGL3-control had poorer transfection efficiency with than without an assisting magnetic force. The probable explanation is that the large amount of internalized magnetic iron oxide under a magnetic field caused the damage of U87 cells because there was no FBS in the culture medium (Supporting Information Figure S4B). On the contrary, the cells looked healthy when there was FBS in the culture medium (Supporting Information Figure S4D). Without applying a magnetic force to the cells, the cell morphology was intact (Supporting Information Figure S4A,B). It was found that the internalized MNP effect on cell damage with or without FBS was more serious in the U87 cells than in the 293T cells when compared with the difference in magnitude of the relative light units between Figures 5 and 7.

Figure 8 clearly shows that the Cy5-labeled pDNA entered the perinuclear region and escaped internalization by the endolysosomes within the 4 h of incubation. Thus, the delivery of more pDNA into the nuclei can be expected when the transfection time is extended. The assistance of a magnetic force indeed increased the intracellular delivery of pDNA into the cytoplasm.

## 5. CONCLUSION

We have shown that previously synthesized PAAIO can be used as a magnetoplex after being coated with PEI. This PEI-PAAIO/pDNA was stable and performed better than PEI and PolyMag as a gene delivery vector because of its lower cytotoxicity. Although transgene expression was lower when FBS was present, when exposed to a magnetic field, the PEI-PAAIO/pDNA showed increased gene transfection efficiency. A key benefit of using this magnetoplex clinically is its resistance to disruption from serum proteins. A magnetofection


dx.doi.org/10.1021/la204529u | *Langmuir* 2012, 28, 3542−3552

technique seems attractive for improving low transfection efficiency in the physiological condition.

## ■ ASSOCIATED CONTENT

### Supporting Information

One table and four figures. This material is available free of charge via the Internet at http://pubs.acs.org.

## ■ AUTHOR INFORMATION

### Corresponding Author

*Tel: 011-886-7-312-1101 ext. 2217. Fax: 011-886-7-312-5339. E-mail: lfwang@kmu.edu.tw.

## ■ ACKNOWLEDGMENTS

We are grateful for the financial support from the National Science Foundation of Taiwan under the grant number of NSC-98-2221-E037-001-MY3, and the Kaohsiung Medical University Research Foundation.

## ■ REFERENCES

(1) Aanton, M.; Plank, C.; Rojo, E. *J. Gene Med.* **2000**, *2*, 66−70.
(2) Huth, S.; Lausier, J.; Gersting, S. W.; Rudolph, C.; Plank, C.; Welsch, U.; Rosenecker, J. *J. Gene Med.* **2004**, *6*, 923−936.
(3) Buerli, T.; Pellegrino, C.; Baer, K.; Lardi-Studler, B.; Chudotvorova, I.; Fritschy, J. M.; Medina, I.; Fuhrer, C. *Nat. Protoc.* **2007**, *2*, 3090−3101.
(4) Shi, Y.; Zhou, L.; Wang, R.; Pang, Y.; Xiao, W.; Li, H.; Su, Y.; Wang, X.; Zhu, B.; Zhu, X.; Yan, D.; Gu, H. *Nanotechnology* **2010**, *21*, 115103.
(5) Pickard, M.; Chari, D. *Nanomedicine (Lond.)* **2010**, *5*, 217−232.
(6) Mykhaylyk, O.; Zelphati, O.; Rosenecker, J.; Plank, C. *Curr. Opin. Mol. Ther.* **2008**, *10*, 493−505.
(7) Ke, J. H.; Lin, J. J.; Carey, J. R.; Chen, J. S.; Chen, C. Y.; Wang, L. F. *Biomaterials* **2010**, *31*, 1707−1715.
(8) Lin, J. J.; Chen, J. S.; Huang, S. J.; Ko, J. H.; Wang, Y. M.; Chen, T. L.; Wang, L. F. *Biomaterials* **2009**, *30*, 5114−5124.
(9) Mazzucchelli, S.; Colombo, M.; De Palma, C.; Salvade, A.; Verderio, P.; Coghi, M. D.; Clementi, E.; Tortora, P.; Corsi, F.; Prosperi, D. *ACS Nano* **2010**, *4*, 5693−5702.
(10) Wang, L.; Neoh, K. G.; Kang, E. T.; Shuter, B.; Wang, S. C. *Biomaterials* **2010**, *31*, 3502−3511.
(11) Malek, A.; Merkel, O.; Fink, L.; Czubayko, F.; Kissel, T.; Aigner, A. *Toxicol. Appl. Pharm.* **2009**, *236*, 97−108.
(12) Merkel, O. M.; Beyerle, A.; Librizzi, D.; Pfestroff, A.; Behr, T. M.; Sproat, B.; Barth, P. J.; Kissel, T. *Mol. Pharmaceutics* **2009**, *6*, 1246−1260.
(13) Liu, Z.; Zheng, M.; Meng, F.; Zhong, Z. *Biomaterials* **2011**, *32*, 9109−9119.
(14) Plank, C.; Rosenecker, J. *CSH Protoc.* **2009**, *2009*, pdb prot5230.
(15) Mykhaylyk, O.; Zelphati, O.; Hammerschmid, E.; Anton, M.; Rosenecker, J.; Plank, C. *Methods Mol. Biol.* **2009**, *487*, 111−146.
(16) Schweiger, C.; Pietzonka, C.; Heverhagen, J.; Kissel, T. *Int. J. Pharm.* **2011**, *408*, 130−137.
(17) Park, J. W.; Bae, K. H.; Kim, C.; Park, T. G. *Biomacromolecules* **2011**, *12*, 457−465.
(18) Ma, Y.; Zhang, Z.; Wang, X.; Xia, W.; Gu, H. *Int. J. Pharm.* **2011**, *419*, 247−254.
(19) Ang, D.; Nguyen, Q. V.; Kayal, S.; Preiser, P. R.; Rawat, R. S.; Ramanujan, R. V. *Acta Biomater.* **2011**, *7*, 1319−1326.
(20) Mykhaylyk, O.; Antequera, Y. S.; Vlaskou, D.; Plank, C. *Nat. Protoc.* **2007**, *2*, 2391−2411.
(21) Namgung, R.; Singha, K.; Yu, M. K.; Jon, S.; Kim, Y. S.; Ahn, Y.; Park, I. K.; Kim, W. J. *Biomaterials* **2010**, *31*, 4204−4213.
(22) Chertok, B.; David, A. E.; Yang, V. C. *Biomaterials* **2010**, *31*, 6317−6324.
(23) Isalan, M.; Santori, M. I.; Gonzalez, C.; Serrano, L. *Nat. Methods* **2005**, *2*, 113−118.
(24) Briley-Saebo, K.; Bjornerud, A.; Grant, D.; Ahlstrom, H.; Berg, T.; Kindberg, G. M. *Cell Tissue Res.* **2004**, *316*, 315−323.
(25) Hykrdova, L.; Jirkovsky, J.; Grabner, G.; Mailhot, G.; Bolte, M. *Photochem. Photobiol. Sci.* **2003**, *2*, 163−170.
(26) Lou, Y. L.; Peng, Y. S.; Chen, B. H.; Wang, L. F.; Leong, K. W. *J. Biomed. Mater. Res. A* **2009**, *88*, 1058−1068.
(27) Germershaus, O.; Mao, S.; Sitterberg, J.; Bakowsky, U.; Kissel, T. *J. Controlled Release* **2008**, *125*, 145−154.
(28) Arsianti, M.; Lim, M.; Marquis, C. P.; Amal, R. *Langmuir* **2010**, *26*, 7314−7326.
(29) Veiseh, O.; Gunn, J. W.; Zhang, M. *Adv. Drug Delivery Rev.* **2010**, *62*, 284−304.
(30) Weissleder, R.; Bogdanov, A.; Neuwelt, E. A.; Papisov, M. *Adv. Drug Delivery Rev.* **1995**, *16*, 321−334.
(31) Chorny, M.; Polyak, B.; Alferiev, I. S.; Walsh, K.; Friedman, G.; Levy, R. J. *FASEB J.* **2007**, *21*, 2510−2519.
(32) Shubayev, V. I.; Pisanic, T. R., 2nd; Jin, S. *Adv. Drug Delivery Rev.* **2009**, *61*, 467−477.
(33) Tseng, W. C.; Fang, T. Y.; Su, L. Y.; Tang, C. H. *Mol. Pharmaceutics* **2005**, *2*, 224−232.
(34) Han, S. E.; Kang, H.; Shim, G. Y.; Kim, S. J.; Choi, H. G.; Kim, J.; Hahn, S. K.; Oh, Y. K. *J. Drug Targeting* **2009**, *17*, 123−132.
(35) Wang, Y. Q.; Sun, Y. X.; Hong, X. L.; Zhang, X. Z.; Zhang, G. Y. *Mol. Biosyst.* **2010**, *6*, 256−263.
(36) Chen, L.; Tian, H.; Chen, J.; Chen, X.; Huang, Y.; Jing, X. *J. Gene Med.* **2010**, *12*, 64−76.
(37) Wen, Y.; Pan, S.; Luo, X.; Zhang, X.; Zhang, W.; Feng, M. *Bioconjugate Chem.* **2009**, *20*, 322−332.
(38) Xia, T.; Kovochich, M.; Liong, M.; Meng, H.; Kabehie, S.; George, S.; Zink, J. I.; Nel, A. E. *ACS Nano* **2009**, *3*, 3273−3286.
(39) Rethore, G.; Mathew, A.; Naik, H.; Pandit, A. *Tissue Eng., Part C: Methods* **2009**, *15*, 605−613.
(40) Morris, V. B.; Sharma, C. P. *Int. J. Pharm.* **2010**, *389*, 176−185.
(41) Alshamsan, A.; Hamdy, S.; Samuel, J.; El-Kadi, A. O.; Lavasanifar, A.; Uludag, H. *Biomaterials* **2010**, *31*, 1420−1428.